

Dissociative ionization of N₂ produced by 1-MeV H⁺ and He⁺: Time-energy spectroscopy

A. K. Edwards, R. M. Wood, and M. F. Steuer

Department of Physics and Astronomy, University of Georgia, Athens, Georgia 30602

(Received 20 August 1976)

By measuring the energy and time of flight of fragment ions from molecular breakup, the fragments can be separated according to their mass to charge ratios and the kinetic-energy spectra for each recorded. This technique is applied to the dissociative ionization of N₂ caused by 1-MeV H⁺ and He⁺ projectiles. The energy spectra for N⁺ is not unlike that produced by electron bombardment, but the N⁺⁺ spectra show some high-energy structure that has not been previously observed. An N³⁺ spectrum is obtained with a maximum near 25 eV, and the reflection method is used to obtain a potential curve for a presumed N₂³⁺ state.

INTRODUCTION

A new technique has been developed to investigate the dissociative ionization of molecules caused by ion bombardment. The method, which has been described in detail elsewhere,¹ uses both time-of-flight (TOF) and electrostatic energy analysis to measure energy spectra of the various mass-to-charge ratio fragments that are produced. Dissociative ionization of N₂ has been investigated by electron scattering studies²⁻⁸ with measurements of kinetic energy, angular distribution, and appearance potentials of the fragments. Other measurements have been made by accelerating N₂⁺ ions and observing their break-up in flight,⁹ or observing their dissociation upon collision with a target gas.¹⁰⁻¹²

More recently, measurements have been made using beams of H⁺ at 100-keV energy¹³ and H⁺ and He⁺ at 5-keV energy.¹⁴ These results showed only a single energy spectrum produced by all fragments. No attempt was made to separate the various charge states of the N ions. By measuring the TOF to and through the electrostatic analyzer, the different charge states of the fragments can be investigated separately.

EXPERIMENTAL PROCEDURE

Figure 1 is a schematic of the apparatus and electronics. Beam pulses from the University of Georgia Van de Graaff accelerator, typically 100 nsec wide, pass through a differentially pumped collision chamber containing the N₂ target gas. The fragments formed in the dissociative processes and ejected at 90° from the beam direction are focused onto the entrance slit of a parallel-plate electrostatic analyzer. A channeltron detector is positioned at the exit of the analyzer. The energy resolution of the analyzer is approximately 0.5% and all fragments are preaccelerated to be analyzed at the same energy (typically 50 eV for singly charged ions). The flight path for the TOF measurements is about 5 cm before acceleration and about 15 cm after acceleration. The entire path is coated with carbon soot to reduce contact potentials and the reflection of particles from surfaces. The system is surrounded by three sets of mutually perpendicular Helmholtz coils to reduce the Earth's and stray magnetic fields.

Timing signals are generated by the beam pulses passing through a capacitive pick-off unit placed before the collision region. The beam-pick-off

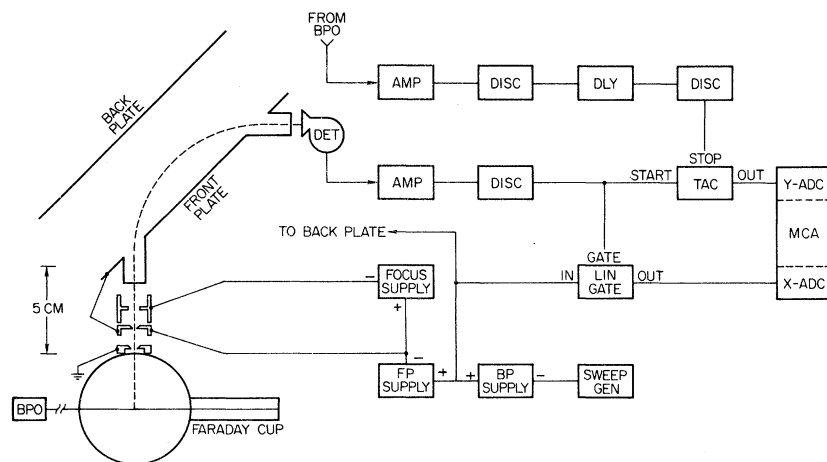


FIG. 1. Schematic of the apparatus and electronics used to obtain the kinetic energy spectra of fragment ions.

(BPO) signal is used to stop a time-to-amplitude converter (TAC) which is started by a channeltron pulse. The TAC output is a signal whose amplitude is linearly related to the TOF of the ion. It is recorded on the Y axis of a 64×64 array of a multichannel analyzer (MCA).

The x coordinate is the voltage on the back plate of the electrostatic analyzer which corresponds to the particle's energy at the time a particle is detected by the channeltron. The back plate is swept continuously by a triangular wave generator. Not shown in Fig. 1 are delays and other circuit elements included to insure that the signal to the x and y axes of the MCA arrive simultaneously for proper storage in the 64×64 array.

DATA REDUCTION

The data displayed by the MCA are curves of the form

$$T = K_1 - K_2(m/q)^{1/2}E^{-1/2} - K_3(m/q)^{1/2}, \quad (1)$$

where K_1 , K_2 , and K_3 are constants which depend on the phase of the BPO signal, flight-path geometry and accelerating voltages. The energy, mass, and charge of the ions are E , m , and q , respectively. A curve is obtained for each charge state of the N fragments as shown in Fig. 2. The discontinuity in the N^+ curve is due to the choice of repetition rate and timing adjustments. Equation (1) can be fitted to the maxima in intensity of the data curves and the mass-to-charge ratio of the fragments for each curve determined.

The energy spectrum for each fragment is obtained from the 64×64 -channel array in the following manner: For each channel on the x axis (energy) a sum is taken over the group of y -axis (TOF) channels corresponding to a particular fragment. The summing is done after subtracting background. Typical spectra are shown in Figs. 3-6.

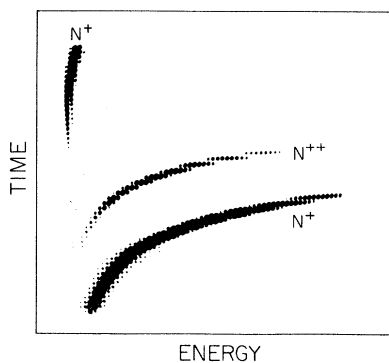


FIG. 2. Display for 1-MeV He⁺ on N₂. The ordinate is T and the abscissa is energy/charge. Each curve corresponds to a different charge state (m/q) of N .

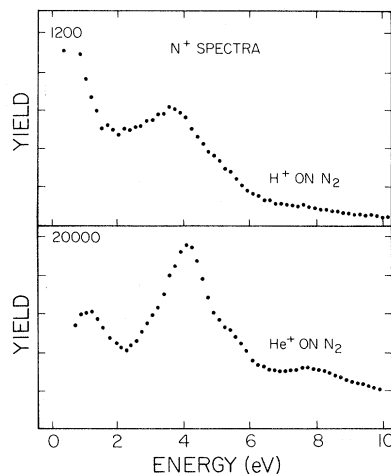


FIG. 3. Kinetic energy spectra of N^+ produced by 1-MeV H^+ and He^+ .

The error bars in these figures indicate statistical uncertainties.

RESULTS

The maxima in the kinetic energy spectra of the various charge states of N are listed in Table I. The errors listed are estimated from the measured sample standard deviations. The N^+ spectra produced by both H^+ and He^+ are shown in Fig. 3. The results are generally in good agreement with the 100-keV H^+ work of Crooks and Rudd¹³ except at low energies where Fig. 3 shows a rise and their results are decreasing. Also, the 7.6-eV structure of their work is not discernible here. These two discrepancies imply an energy (or velocity) dependence for the excitation cross section. The results of Seibt¹² are from 20-keV N_2^+ on He collisions. The low-energy maximum in the N^+ spectrum (0.7 eV for H^+ and 1.0 eV for He^+) is believed to be produced by dissociation from the

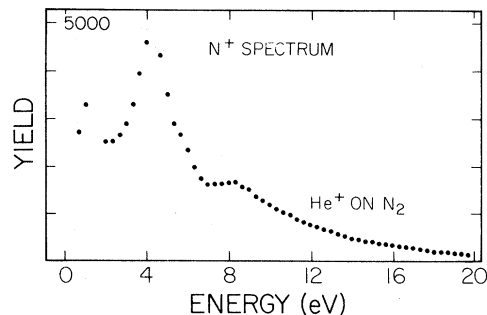


FIG. 4. Kinetic energy spectra of N^+ produced by He^+ showing the high-energy tail.

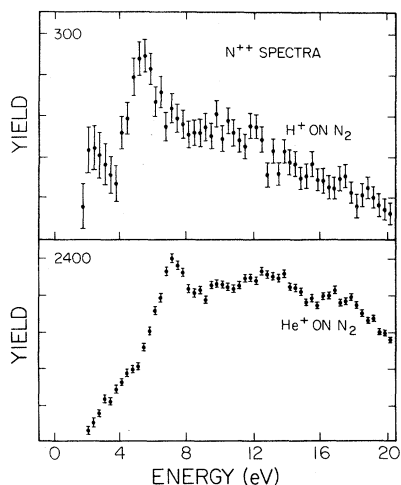


FIG. 5. Kinetic energy spectra of N^{++} produced by 1-MeV H^+ and He^{++} .

$C^2\Sigma_u^+$ of N_2^+ as shown by Fournier *et al.*¹¹ This experiment does not have the resolution to show vibrational structure.

The 3.8-eV dissociation energy for N^+ produced by H^+ projectiles is believed to be from the $D^2\Pi_g$ level¹⁵ of N_2^+ . For low-energy N_2^+ -on- N_2 collisions,¹⁰ dissociation from this state was found to be dominant. With the He^+ beam the maximum in this energy region is enhanced and peaks at 4.2 eV. This enhancement may be due to an added contribution from the dissociation process $N_2^{++} \rightarrow N^+(^3P) + N^+(^3P)$. A potential curve of N_2^{++} with a dissociation energy in this region which could contribute is the $A^3\Pi_g$ calculated by Hurley.¹⁶ Higher charge states of the fragments are more readily formed by the He^+ beam than the H^+ beam.

Electron excitation works²⁻⁸ report structure

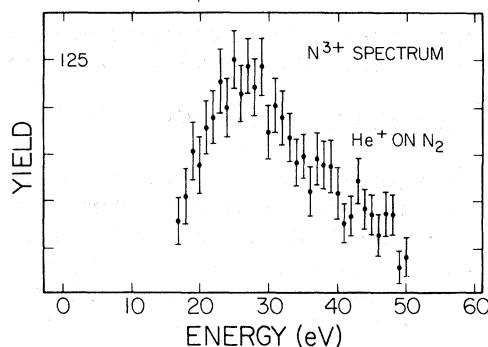


FIG. 6. Kinetic energy spectrum of N^{3+} produced by 1-MeV He^+ .

similar to that presented here plus other maxima in the 2-3-eV region. For the He^+ beam a long high-energy tail is observed in the N^+ spectrum and is shown in Fig. 4. This may be due mostly to $N_2^{++} \rightarrow N^+ + N^+$ breakup. Higher charge states of N_2 can contribute but they are more weakly excited.

The N^{++} spectra produced by H^+ and He^+ are shown in Fig. 5. The N^{++} is more readily formed by the He^+ projectile. Crowe and McConkey⁵ report maxima of 2.9, 5.1, and 7.9 eV for N^{++} produced by 300-eV electrons-on- N_2 collisions. Similar structure is seen by Stockdale and Deleanu.⁴ The structure above 10 eV has not been reported in the electron excitation measurements and may be due to $N_2^{3+} \rightarrow N^{++} + N^+$ breakup.

The N^{3+} spectrum produced by He^+ is shown in Fig. 6. The reflection method¹⁷⁻¹⁹ has been used to deduce a potential curve for the state through which the N^{3+} fragments are formed. The measured values of the intensity were assumed to be

TABLE I. Maxima in the kinetic energy spectra of N^+ , N^{++} , and N^{3+} produced by heavy-particle collisions.

Fragment	This work		Maxima (eV)		Fournier ^c <i>et al.</i>
	H^+	He^+	Crooks and Rudd ^a	Seibt ^b	
N^+	0.7 ± 0.2	1.0 ± 0.2			0.03-1.44
	3.8 ± 0.2	4.2 ± 0.2	3.85	3.42	
	5.0 ± 0.2	5.7 ± 0.3	5.0		
		8.0 ± 0.2	7.6		
N^{++}	2.3 ± 0.5	4.2 ± 0.5			
	5.3 ± 0.3	6.6 ± 0.3			
	10.2 ± 0.5	12.1 ± 0.5			
		16.0 ± 0.6			
N^{3+}		25 ± 1.0			

^aReference 13.

^bReference 12.

^cReference 11.

an accurate representation of the true energy-distribution function $N(E)$. Normalization requires

$$\int_0^{\infty} \eta N(E) f(E) dE = 1 = \int_0^{\infty} \bar{M}^2 S^2 \chi^2(x) dE,$$

where \bar{M} is the electronic transition moment, S is a normalization function for the repulsive state,¹⁷ $\chi(x)$ is the normalized eigenfunction for the initial N₂ state, η is a normalization factor, $f(E)$ is the energy distribution function for the electrostatic analyzer, and x is the displacement from the equilibrium separation of 1.094 Å for N₂.²⁰

Since the n th channel value of the measured intensity, N_n , is assumed equal to $[N(E)f(E)w]_n$, where w is the channel width, we obtain

$$N_n = \bar{M}^2 S_n^2 \chi(x) f(E) w \eta^{-1} \quad (2)$$

and

$$S_n/S_{n'} = (E_n/E_{n'})^{1/4},$$

where n' refers to the channel number selected for normalization. The ground-state wave function is represented by

$$\chi(x) = (\alpha/\pi)^{1/4} e^{-\alpha x^2/2} \quad (3)$$

where $\alpha = 487 \text{ \AA}^{-2}$ as obtained from Herzberg.²⁰ From Eqs. (2) and (3) it follows that

$$x_n^2 - x_{n'}^2 = (1/\alpha) \ln[(N_n/N_{n'})(E_n/E_{n'})^{1/2}], \quad (4)$$

which has a minimum at the equilibrium separation ($x_n = 0$).

A smooth curve was drawn through the data, and the value at 17 eV was arbitrarily chosen as the normalization value $N_{n'}$. The data were then used to compute the values of the function of Eq. (4). These values were plotted and a smooth curve was drawn through the resulting points. The energy of the minimum value of the function was established

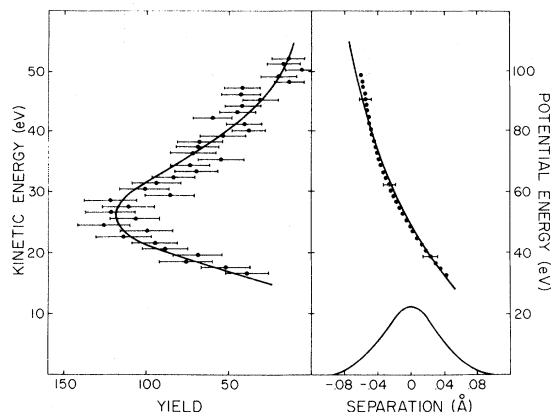


FIG. 7. Kinetic energy spectrum of N³⁺ together with the potential deduced from the data using the reflection method. The bell-shaped curve in the lower right-hand corner is the ground-state N₂ curve. Directly above it is the deduced potential curve and to the left is the measured N³⁺ spectrum. The solid curves through the data and potential were calculated using a simple r^{-11} potential.

to be 25 ± 1.0 eV. This energy corresponds to $x = 0$.

Equation (4) was then used to calculate the value of x_n for each channel. Since the energy of each channel was known and since the potential energy at each point is twice the kinetic energy of the detected ion, the potential energy was determined corresponding to each of the deduced x values. The results are the dotted points shown in Fig. 7. An estimate of the probable error is given at three selected points. The solid potential curve is a simple r^{-11} potential which was the best fit to the potential deduced from the data for any integer power of r . The solid curve representing $N(E)$ was computed from the r^{-11} potential.

¹R. M. Wood, A. K. Edwards, M. F. Steuer, Rev. Sci. Inst. (to be published).

²H. D. Hagstrum, Rev. Mod. Phys. **23**, 185 (1951).

³L. J. Kieffer and R. J. Van Brunt, J. Chem. Phys. **46**, 2728 (1967); J. Chem. Phys. **63**, 3216 (1975).

⁴J. A. D. Stockdale and L. Deleanu, Chem. Phys. Lett. **22**, 204 (1973); J. Chem. Phys. **63**, 3898 (1975).

⁵A. Crowe and J. W. McConkey, J. Phys. B **6**, 2108 (1973); J. Phys. B **8**, 1765 (1975).

⁶K. C. Smyth, J. A. Schiavone, and R. S. Freund, J. Chem. Phys. **59**, 5225 (1973).

⁷K. Köllmann, Int. J. Mass Spectrosc. Ion Phys. **17**, 261 (1975).

⁸R. Lochter, J. Schopman, H. Warkenne, and J. Momigny, Chem. Phys. **7**, 393 (1975).

⁹P. G. Fournier, T. R. Govers, C. A. Van De Runstraat,

J. Schopman, and J. Los, J. Phys. (Paris) **33**, 755 (1972).

¹⁰T. F. Moran, F. C. Petty, and A. F. Hendrick, J. Chem. Phys. **51**, 2112 (1969).

¹¹P. Fournier, C. A. Van De Runstraat, T. R. Govers, J. Schopman, F. J. Deteer, and J. Los, Chem. Phys. Lett. **9**, 426 (1971).

¹²W. Seibt, *Sixth International Conference on the Physics of Electronic and Atomic Collisions* (MIT Press, Cambridge, 1969), p. 803.

¹³J. B. Crooks and M. E. Rudd, *Ninth International Conference on the Physics of Electronic and Atomic Collisions* (University of Washington Press, Seattle, 1975), p. 755.

¹⁴R. H. McKnight and F. D. Gilliland, Ref. 13, p. 717.

¹⁵F. R. Gilmore, J. Quant. Spectrosc. Radiat. Transfer

5, 369 (1965).

¹⁶A. C. Hurley, *J. Mol. Spectrosc.* 9, 18 (1962).

¹⁷A. S. Coolidge, H. M. James, and R. D. Present, *J. Chem. Phys.* 4, 193 (1936).

¹⁸H. D. Hagstrum and J. T. Tate, *Phys. Rev.* 59, 354

(1941).

¹⁹G. H. Dunn and L. J. Kieffer, *Phys. Rev.* 132, 2109 (1963).

²⁰G. Herzberg, *Spectra of Diatomic Molecules* (Van Nostrand, Princeton, 1950), p. 553.